Citation: Askr M. N., Eraky A., Salama A., et al. Experimental and numerical evaluation of elevated rectangular water tank frequencies using digital image correlation. *Journal of Harbin Institute of Technology (New Series)*. DOI: 10.11916/j.issn.1005-9113.2025046

Experimental and Numerical Evaluation of Elevated Rectangular Water Tank Frequencies Using Digital Image Correlation

Askr M. N. *, *Eraky A*, *Salama A. and Emad S.*

(*Department of Structural Engineering*, *Faculty of Engineering*, *Zagazig University*, *Zagazig 44519*, *Egypt*)

Abstract: Elevated, rectangular water tanks are an essential component of the water supply network and for emergency water storage purposes. However, determining the dynamic response from seismic loads will require good estimates of their natural frequencies to help avoid damage or failure. Several numerical and analytical methodologies depend on assumptions that may not account for the complexity of fluid-structure interaction regarding rectangular geometries, indicating a strong need for solid experimental validation. This study pioneers the application of Digital Image Correlation (DIC), a non-contact optical technique, to measure the natural frequencies of a small-scale acrylic and Teflon tank, addressing this gap with a novel experimental approach. The method includes DIC using a high-speed camera, image analyzed by MATLAB, frequency analysis by Continuous Wavelet Transformation (CWT), and Fast Fourier Transformation (FFT); ANSYS finite element analysis, simplified models based on Eurocode and the Egyptian Code of Practice (ECP). Study results indicate that DIC is critical for attaining large accuracy, with maximum error differing by 2.92% for impulsive and 4.55% for convective frequencies from ANSYS and provides a better measure of dynamic response compared to contact-based measurements. Impulsive frequency decreased from 5.8724 Hz to 4.0085 Hz, and sloshing increased from 1.00 Hz to 1.84 Hz, depending on the changing water cover height from 0 cm to 9.8cm. The Eurocode and ECP models describe acceptable errors of 7.36% and 9.21%, respectively. DIC showed a better level of accuracy, making it a useful tool in seismic design. This study improves the safety and reliability of designs for elevated water tanks in seismic regions with elevated seismic risk.

Keywords: fluid-structure interaction; natural frequency; rectangular tank; elevated tank; sloshing waves; DIC

CLC number: TU317.2 **Document code**: A **Article ID**: 1005-9113(2024)00-0000-12

0 Introduction

Elevated rectangular tanks are critical infrastructure elements of water supply systems, industrial processes, and emergency storage solutions, which are intended to store fluids at elevated levels for necessary durations. Their dynamic response, especially their natural frequencies, is critical to maintain structural integrity and functional reliability against environmental hazards such as earthquakes that can impose severe hydrodynamic loads[1]. The correct prediction of natural frequencies is essential to anticipate resonance phenomena, reduce the risks of structural failure, and improve long-term performance.

Natural frequencies of elevated rectangular tanks have been traditionally calculated using analytical along with numerical methods. The early analytical techniques, as evident from the works of Rayleigh[2] and Timoshenko et al.[3], were based on the application of approximate modes of vibration that could not accurately predict the behavior of actual structures. Modal analysis, though possessing greater accuracy, is limited by assumptions, constraints, and difficulties in dealing with complicated geometries[4]. Numerical investigations, as illustrated by Pal and Bhattacharyya[5], have provided techniques like the Local Symmetric Weak Form (LSWF) for non-linear sloshing analysis of prismatic tanks, which are partially filled. Sahu et al.[1] observed that experimental and analytical methods exhibit little difference in lower modes, but reveal broad divergence in higher modes. Ninan et al.[6] identified differences in mode shapes for circular and rectangular

Received 2025-04-14.

* Corresponding author: Askr M. N., Teaching Assistant. Email: MENasr@eng.zu.edu.eg.

tanks with the shortening of the vibration period by braces. Visuvasam et al.[7] depicted that the fundamental period is affected linearly by soil-structure interaction with significant variation for soft soils. Vimal et al.[8] investigated base isolation, which demonstrated its effect on the base shear and moment, particularly for the higher modes.

Kangda et al.[9] showed that the use of internal baffles in square tanks reduces sloshing amplitudes, a critical factor for the design to be stable. Recent studies, as those by Fang et al.[10] and Sun et al.[11], have developed further in numerical modeling of fluid-structure interaction, proving high accuracy at various water levels and soil conditions, but mostly focused on cylindrical tanks. Despite these developments, a serious knowledge gap exists regarding experimental validation in fluid-structure interaction research with tall rectangular tanks. The majority of investigations are either numerical simulations or reduced analytical models, which carry assumptions that may not precisely reflect actual conditions, especially for rectangular geometries. Traditional experimental devices, such as extensometers and strain gauges, provide localized measurements that can inadvertently affect the structural response and, hence, are not appropriate for small, fragile, or complex specimens. Full-field non-contacting techniques, as the Digital Image Correlation (DIC) method, eliminate this limitation by measuring strain over complete surfaces in a non-contact manner, thus improving spatial data and enabling more accurate results to be achieved[12].

DIC is a possible answer to bridge this gap. As a non-contact optical method, DIC can measure deformation, strain, and displacement very precisely without influencing the test specimen[12]. Its application in structural dynamics, as demonstrated by Montiel et al.[13], Kumar et al.[14], and Zhang et al.[15-16], has been discovered to be of great accuracy in dynamic response capturing. Luo et al.[17] investigated the cracking behavior of Ultra-High Performance Fiber Reinforced Concrete (UHPFRC) using DIC. Among their findings was that superposition techniques could be applied to investigate axial tensile yield and peak load of R-UHPFRC, but may overstate stiffness in the service limit state. Aryanto et al.[18] worked on four concrete beams subjected to loads and reported that DIC is better than conventional techniques, such as strain gauges, because of non-contact measurement, calculation efficiency, and accuracy. Results obtained from DIC helped to detect early fractures and measure crack values, with good conformity to the experimental measurement.

Its application, however, in the determination of the natural frequencies of liquid-filled elevated rectangular tanks remains uncharted. The combination of DIC with high-speed imaging and sophisticated signal processing methodologies, like Continuous Wavelet Transformation (CWT) and Fast Fourier Transformation (FFT), offers a breakthrough stage for linking theoretical predictions with experimental evidence.

This study fills the research gap by experimentally validating the natural frequencies of an elevated rectangular water tank using DIC, supplemented with a high-speed camera to measure sloshing and impulsive frequencies. The novelty lies in the application of DIC for quantifying fluid-structure interaction on a small-scale tank model and comparing it with finite element models (ANSYS) and design code models (Eurocode and Egyptian Code of Practice). With the application of DIC's non-contacting capability, this study provides a low-cost and accurate dynamic response measurement with a valid framework for numerical model validation. This study has a twofold contribution: it validates the effectiveness of DIC in accurately capturing both the impulsive and convective frequencies and also makes an elaborate comparison with the simplified design codes, thereby bringing out their limitations for rectangular tanks. In this way, a better understanding of fluid-structure interaction is provided and a step towards safer and more dependable elevated tank design is contributed.

1 Methodology

The study uses experimental and numerical methods to analyze the natural frequencies of an elevated rectangular water tank, considering the fluid-structure interaction using DIC and finite element analysis. There are three key aspects of the method: experimental test setup, finite element analysis, and simplified modeling using design codes.

1.1 Experimental Setup

The experimental model consists of an elevated rectangular acrylic water tank, supported by Teflon columns. The tank's specifications are summarized in

Table 1. The tank is fixed to the ground using steel bolts to act as a fixed base.

Table 1 Specifications of the tank

Parameter	Value
Material (walls and base)	Acrylic
Material (columns)	Teflon
Dimensions (L×W×H)	25 cm ×20 cm ×20 cm
Wall thickness	5 mm
Base thickness	9 mm
Column height	25 cm
Column diameter	15 mm
Fixing method	Steel bolts to the ground
Elastic modulus (acrylic)	2800 MPa
Elastic modulus (teflon)	382 MPa

For capturing dynamic behavior, a high-speed camera of 240 Frames Per Second (FPS) was employed for the analysis by DIC. The camera was positioned 1.5 m in front of the longitudinal face of the tank, perpendicular to it, to get a clear capture of the whole surface of the tank. A single speckle high-contrast red dot (diameter 2−3 mm) was painted on the tank's outer surface using non-reflective paint to enable precise tracking of the surface movements. The camera was placed on a tripod to reduce vibrations, and two 500W LED lights were used for illumination to remove shadows and make the images clearer.

The experimental method consisted of giving an initial lateral displacement to the tank and letting it be released. To ensure reproducibility, several videos were taken for each of the water levels, ranging from 1.4 cm to 9.8 cm. The taken videos were processed with MATLAB to obtain displacement information by DIC using the following algorithm.

Get the required video; Determine the ordinates of pixels of the point that is to be followed (p1); Search for the ordinates of the pixels matching (p1) throughout each frame; Determine pixel ordinate against time.

The displacement records were then processed by applying CWT and FFT to identify the impulsive and convective frequencies and their corresponding power spectra. Fig.1 illustrates the configuration of the experimental model.

1.2 Finite Element Analysis

The numerical analysis was done with ANSYS Workbench 2023 R1, according to the procedure developed by Anagha et al.[19], to simulate the fluid-structure interaction and calculate the natural frequencies of the tank. The geometry was generated by DesignModeler, reproducing the dimensions and the material properties of the test tank provided in Table 1.

Fig.1 Experimental model

The tank was modeled using SOLID187 elements, which are mid-side node third-order 3D tetrahedral elements having three translational degrees of freedom (x, y, z) per node. The fluid domain was discretized using FLUID220 elements, having translations in the x, y, and z directions and pressure, with an FSI (Fluid-Structure Interaction) flag at the interface between the tank and the fluid to couple structural and acoustic response. The contact between fluid and tank walls was modeled using CONTA174 and TARGE170 elements to define contact behavior, where the tank surface was defined as deformable and the fluid interface as a rigid target. To ensure accuracy, the mesh was refined to an element size of 7.5 mm for the tank walls and fluid domain, and 2.5 mm for the columns. This results in approximately 100, 000 elements for the tank, with the fluid domain's element count varying based on its height. A convergence check confirmed the mesh produced stable frequency results with less than a 1% discrepancy from finer meshes. To correctly represent the bolt connection at the base of the Teflon columns, a fixed boundary condition was used. In convective frequency analysis, the free surface boundary condition was specified on the upper surface of the fluid, with gravitational acceleration of 9.81 m/s^2 to represent the sloshing effects. In impulsive frequency analysis, pressure on the upper surface of the fluid was maintained at 0 Pa. Modal analysis for the empty tank was done using the standard modal method, whereas fluid-filled tanks were analyzed using Modal Acoustics to identify both impulsive and convective modes. Fig. 2 presents the ANSYS model of the empty tank, whereas Fig. 3(a) and 3(b) present the Modal Acoustics setup for impulsive and convective

frequencies, respectively.

1.3 Simplified Modeling

Simplified models were created based on Eurocode and the Egyptian Code of Practice (ECP) to simulate the dynamic behavior of the tank. The Eurocode approach uses lumped mass models where the tank-liquid system is represented by two single-degree-of-freedom systems: one for the impulsive component (traveling with the tank walls) and the other for the convective component (sloshing). The impulsive mass (m_i), convective mass (m_c), and their respective heights (h_i, h_c) were calculated using the following equations adapted from Eurocode-8 Part 4[20], as illustrated as follows:

$$m_{cn} = m\frac{2\tanh(\lambda_n\gamma)}{\gamma\lambda_n(\lambda_n^2-1)} \tag{1}$$

where m_{cn} is convective mass of n mode, m is water mass, and λ_n is a dimensionless wave number.

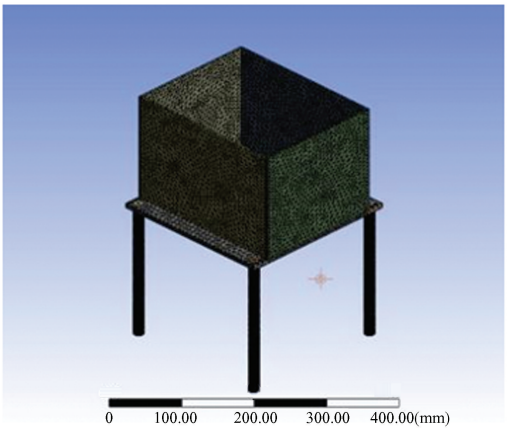

Fig.2 ANSYS model of an empty tank

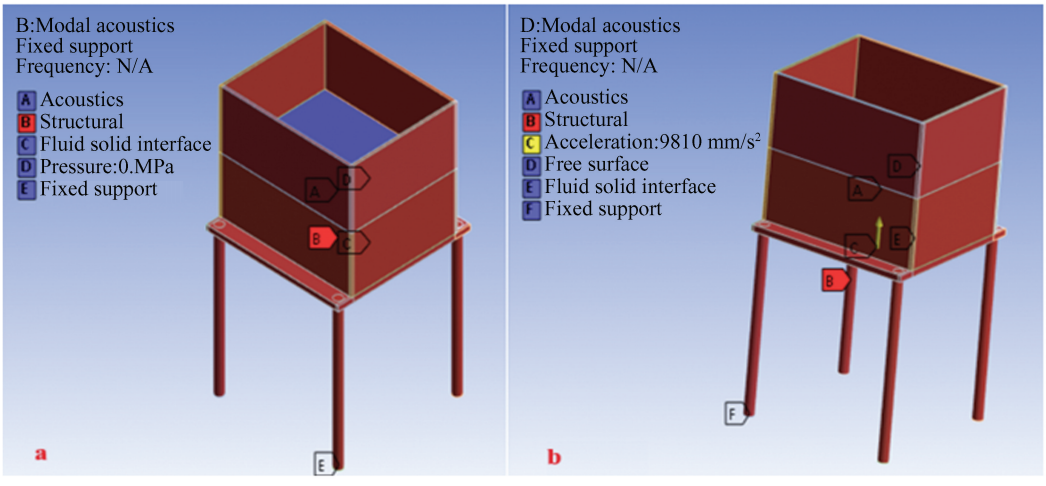

Fig.3 Modal acoustics setup (a) impulsive and (b) convective frequencies

$$h_{cn} = h\left(1+\frac{1-\cosh(\lambda_n\gamma)}{\lambda_n\gamma\sinh(\lambda_n\gamma)}\right) \tag{2}$$

where h_{cn} is the convective mass height of n mode, h is the water height, and λ_n is a dimensionless wave number.

$$\omega_{cn} = \sqrt{g\frac{\lambda_n}{R}\tanh(\lambda_n\gamma)} \tag{3}$$

where ω_{cn} is the convective angular frequency of n mode, λ_n is a dimensionless wave number, γ is the tank slenderness ratio defined in equation 8, g is ground acceleration.

While impulsive mass and corresponding impulsive height can be obtained by Eq.(4).

$$m_i = m2\gamma\sum_{n=0}^{\infty}\frac{I_1(\frac{v_n}{\gamma})}{v_n^3 I'_1(\frac{v_n}{\gamma})} \tag{4}$$

where m_i is impulsive mass, I is the Bessel function, I' is the Bessel function derivative, γ is the tank slenderness ratio defined in Eq. (8), and ν_n is a dimensionless frequency parameter for impulsive mode shapes given by Eq.(6).

$$h_i = h\frac{\sum_{n=0}^{\infty}\frac{(-1)^n I_1\left(\frac{v_n}{\gamma}\right)}{v_n^4 I'_1\left(\frac{v_n}{\gamma}\right)}(v_n(-1)^n-1)}{\sum_{n=0}^{\infty}\frac{I_1(\frac{v_n}{\gamma})}{v_n^3 I'_1(\frac{v_n}{\gamma})}} \tag{5}$$

h_i is the impulsive mass height.

Eq. (6) gives the dimensionless frequency parameter for impulsive mode shapes.

$$v_n = \frac{2n+1}{2}\pi \tag{6}$$

Eq.(7) gives the tank slenderness ratio (also known as aspect ratio).

$$\gamma = \frac{H}{R} \tag{7}$$

where λ_n is a dimensionless wave number, $\lambda_1 = 1.841$, $\lambda_2 = 5.331$, $\lambda_3 = 8.536$, and so on

Although the equations were primarily developed for circular tanks, they can be adapted for rectangular tanks by replacing the radius (R) with the length (L). However, as noted in Eurocode 2006 Part 4, this adaptation may introduce errors of up to 15%.

Also, the period of oscillation of the first sloshing mode of the rectangular tanks has a defined equation, as shown as follows:

$$T = 2\pi \left(\frac{L/g}{\frac{\pi}{2}\tanh\left(\frac{\pi}{2}\frac{H}{L}\right)} \right)^{1/2} \tag{8}$$

where L is half the tank length in the studied direction, g is the ground acceleration, H is the water height in the tank.

The ECP adopts a similar lumped mass approach, using graphical charts to determine convective and impulsive masses and heights for rectangular tanks[21]. The tank was modeled as a two-mass system, with the convective mass connected by springs and the impulsive mass distributed uniformly across the tank walls at the flexible height h_f, as per the third method described in Ref.[22]. The structure was modeled using SAP2000 to compute theoretical fundamental frequencies for both empty and partially filled tanks. Fig. 4 shows the ECP charts for dynamic parameters, Fig. 5 illustrates the two-mass model, and Figs. 6 and 7 depict the SAP2000 models for the empty and partially filled tanks.

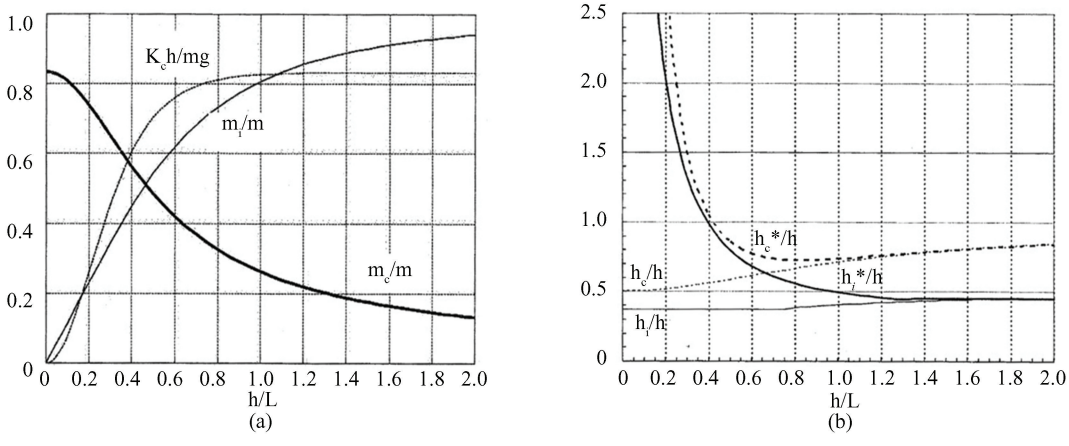

Fig. 4 ECP charts for dynamic parameters: (a) convective and impulsive masses and convective stiffness for rectangular tank, (b) convective and impulsive masses heights for rectangular tank

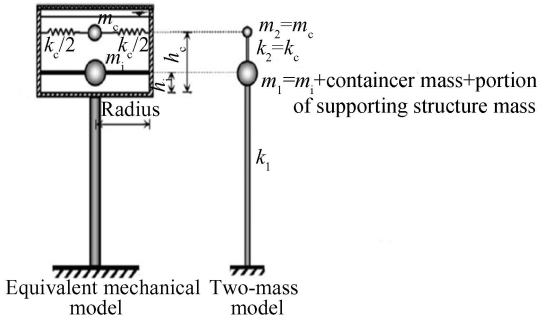

Fig. 5 Elevated tanks two-mass model

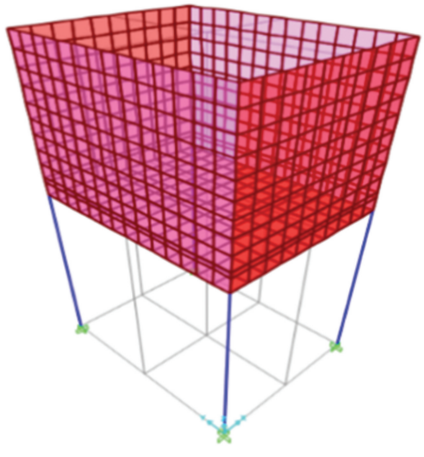

Fig. 6 Finite element model of an empty tank

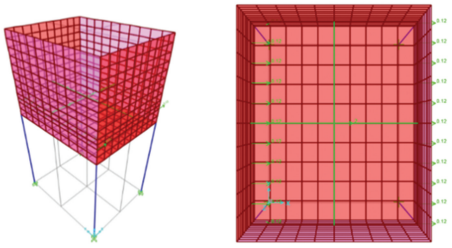

Fig. 7 Finite element model of the partially filled tank (water modeled as impulsive and convective masses)

2 Results and Discussion

This section provides a comprehensive comparison of experimental, numerical, and simplified modeling results of natural frequencies of an elevated rectangular water tank considering fluid-structure interaction. The experimental measurements were acquired through DIC using MATLAB, numerical analysis was made through ANSYS, whereas simplified models were established as per Eurocode and the Egyptian Code of Practice (ECP). The outcomes are examined to compare the accuracy and limitations of each technique.

2.1 Lab Results

Experimental procedures involved rigidly attaching the tank to a solid base and applying an initial lateral displacement to cause free vibration. Slow-motion video at 240 frames per second was recorded using a high-speed camera, which was later analyzed using MATLAB to obtain displacement information through DIC. To enhance reliability, several recordings were obtained at each of the specified water heights, which varied from 0 cm (dry) to 9.8 cm (approximately half full). Fig. 8 presents the maximum sloshing height of two various water levels: (a) water height (hw) is 5 cm (approximately one-quarter full) and (b) water height (hw) 9.8 cm. Higher water levels were seen to be correlated with amplification of sloshing amplitude, indicating greater liquid-structure interaction. The trend validates the significance of accurately modeling sloshing dynamics for tank design.

A 9.8 cm water height displacement-time history, obtained using DIC pixel tracking, is shown in Fig. 9. It has an oscillatory motion with decreasing amplitude, which is a feature of free damped vibration. Over 10 s, the initial displacement decreases, demonstrating the energy loss due to fluid viscosity and structural damping. Frequency analysis is based on this.

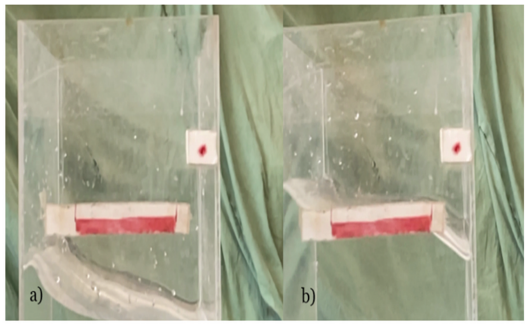

(a) hw=5cm (b) hw=9.8cm

Fig. 8 Maximum sloshing height of tank partially filled with water (a) hw = 5cm, (b) hw = 9.8cm

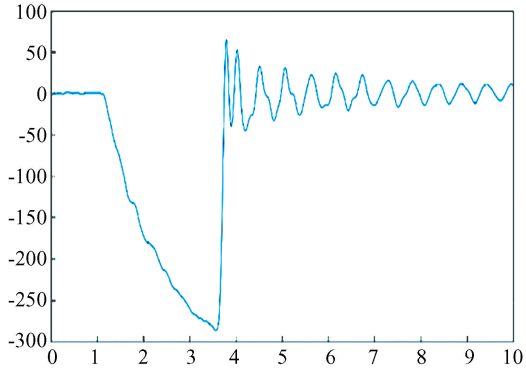

Fig.9 Displacement over time of a tank partially filled with water (hw = 9.8cm)

CWT was used to convert displacement data into the frequency domain. Fig. 10 displays the 3D CWT plot for the 9.8cm level. The axes represent frequency on a logarithmic scale (Hz), time (s), and amplitude in arbitrary units with a color bar for reference. The plot shows the difficulty of detecting the frequencies.

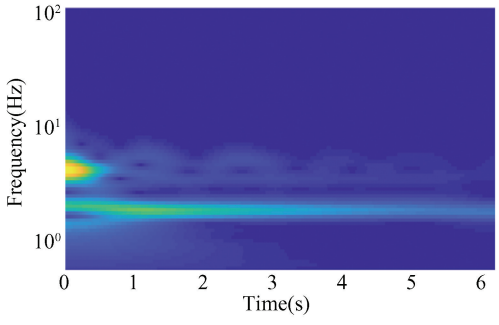

Fig.10 CWT of tank partially filled with water (hw = 9.8cm)

To differentiate the frequencies, CWT sections were analyzed. Figs. 11 and 12 present sections for

water heights, where Fig. 11 for heights from 1.4 cm to 5 cm, with subfigures (a) through (d) for 1.4 cm, 2.6 cm, 3.8 cm, and 5 cm, respectively. Every subfigure detects the impulsive and sloshing frequency of different water heights. More than one section were taken to ensure the accuracy of the analysis, demonstrating decreasing impulsive frequency from 5.84 Hz to 5.11 Hz with increasing water height, echoing the effect of additional liquid mass decreasing structural frequency. Sloshing frequency increases from 1 Hz to 1.63 Hz, fueled by a shallower water depth amplifying wave motion.

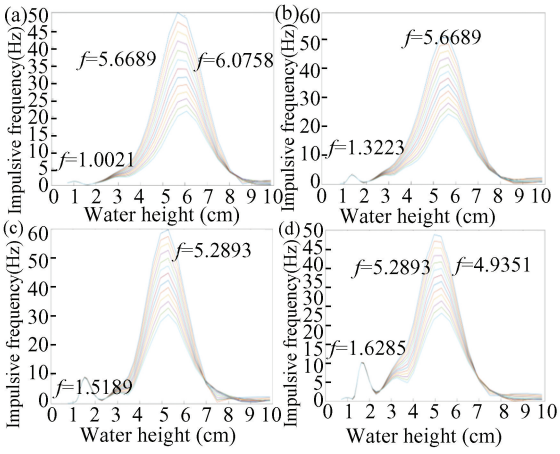

Fig.11 Sections of CWT of tank partially filled with water (a) hw=1.4cm, (b) hw=2.6cm, (c) hw=3.8cm and (d) hw=5cm

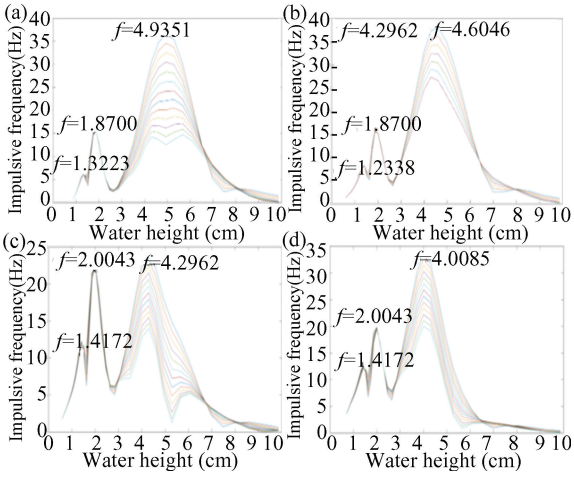

Fig.12 Sections of CWT of tank partially filled with water (a) hw=6.1cm, (b) hw=7.3cm, (c) hw=8.6cm and (d) hw=9.8cm

Fig. 12 demonstrates water height from 6.1 cm to 9.8 cm, with subplots for 6.1 cm, 7.3 cm, 8.6 cm, and 9.8 cm. These plots show impulsive frequency dropping from 4.94 Hz to 4.01 Hz, whereas sloshing frequency rises to 1.84 Hz, though double peaks at high amplitudes show initial water motion disturbance, which possibly caused by turbulent flow or boundary reflections.

To accurately determine the sloshing frequency of the water, FFT was employed to isolate sloshing modes as impulsive frequencies decay, resulting in a single narrow peak, illustrating FFT's capability for determining steady-state frequencies, as shown in Fig.13.

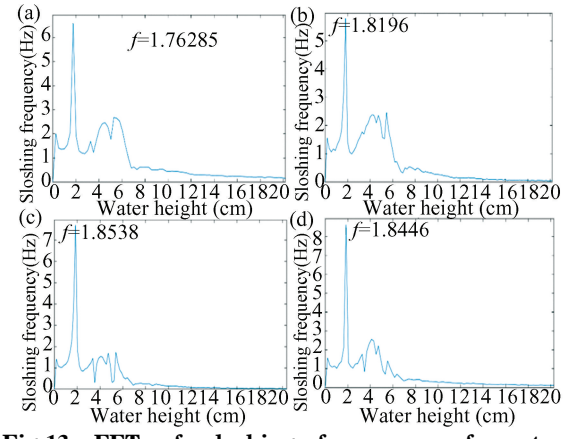

Fig.13 FFT of sloshing frequency of a tank partially filled with water (a) hw=6.1cm, (b) hw=7.3cm, (c) hw=8.6cm, and (d) hw=9.8cm

Table 2 provides experimental frequencies, decreasing base frequency from 5.8724 Hz (void) to 4.0085 Hz at 9.8 cm, and increasing sloshing frequency from 1 Hz to 1.84 Hz, with a diminishing rate of increase as the water depth reaches half of the tank height, reflecting asymptotic behavior in sloshing dynamics. F1 in Table 2 stands for the first (fundamental) sloshing frequency.

Table 2 Frequency with different water heights

h_w (cm)	h_w/L	Lab	
		Frequency (Hz)	Sloshing frequency (Hz) (F1)
No water	0	5.87	--
1.4	0.07	5.84	1.00
2.6	0.13	5.67	1.32
3.8	0.19	5.29	1.52
5.0	0.25	5.11	1.63
6.1	0.305	4.94	1.76
7.3	0.365	4.45	1.82
8.6	0.43	4.30	1.85
9.8	0.49	4.01	1.84

2.2 Finite Element Results

2.2.1 ANSYS results

The ANSYS model for the empty tank, using material properties (Teflon: 382 MPa, acrylic: 2800

MPa) and experimental dimensions, produced a fundamental frequency of 5.9005 Hz in the motion direction, with a 0.48% error compared to the experimental 5.8724 Hz. Fig. 14 shows the first mode shape, confirming the model's accuracy for the empty tank. The low error suggests accurate modeling of structural stiffness and mass distribution.

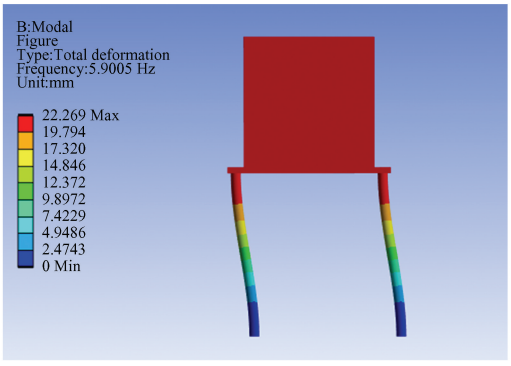

Fig.14 ANSYS model: Frequency of empty tank

Fluid-filled tank models were analyzed to help compare impulsive and convective frequencies with experimental measurements. Table 3 is an example of a comparison of the ANSYS results with the experimental results at every water level. The ANSYS results provided a maximum of 2.92% error for impulsive frequencies on the water level of 7.3 cm and a maximum of 5% error for convective frequencies on the water level of 1.4 cm and demonstrate precision with respect to experimental measurements. The errors are likely linked to assumptions made in the comparison, i.e., ideal boundary conditions or finite mesh resolutions used for the fluid tank simulation. Fig. 15 compares experimental results to ANSYS results with respect to the fluid frequencies. The experimental measurements and ANSYS results correlate very well with each other, particularly at lower heights. This provides validation for DIC precision. The discrepancy between the ANSYS results and experimental results at 3.8 cm and 7.3 cm may be due to the camera frame rate (240 Hz) or the resolution of speckle patterns that affected the DIC accuracy.

Table 3 Convective and impulsive frequencies using ANSYS in comparison with lab results

h_w (cm)	Lab		Model ANSYS		Error (Model ANSYS) (%)	
	Impulsive frequency (Hz)	Sloshing frequency (Hz)	Impulsive frequency (Hz)	Sloshing frequency (Hz)	Impulsive frequency (%)	Sloshing frequency (%)
No water	5.87	--	5.9	--	0.51	--
1.4	5.84	1.00	5.82	0.95	0.34	5.00
2.6	5.67	1.32	5.66	1.26	0.18	4.55
3.8	5.29	1.52	5.42	1.47	2.46	3.29
5.00	5.11	1.63	5.14	1.6	0.59	1.84
6.1	4.94	1.76	4.87	1.69	1.42	3.98
7.3	4.45	1.82	4.58	1.75	2.92	3.85
8.6	4.3	1.85	4.29	1.79	0.23	3.24
9.8	4.01	1.84	4.02	1.81	0.25	1.63

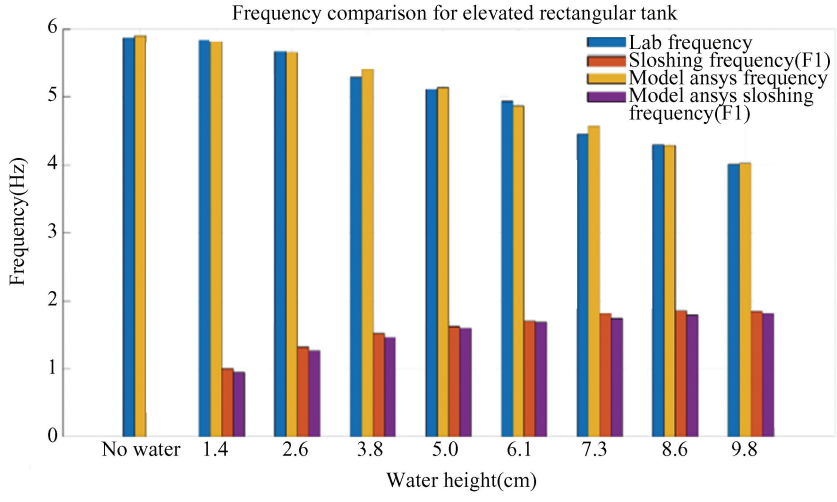

Fig.15 Comparison between experimental and numerical frequencies

2.2.2 Simplified results

A variety of simplified models were developed employing the Eurocode and ECP, allowing for estimating the dynamic behavior and offering practical alternatives to complicated numerical-based simulations. The empty tank model, with the same properties as ANSYS, produced a fundamental frequency of 5.92023 Hz in the X-direction, as in Fig.16, which shows an error of 0.8145% compared to the experimental value of 5.8724 Hz, indicating good correlation despite simplified assumptions.

2.2.3 Model data acquisition

Using equations given in the Eurocode and the graphs given in ECP, the models data were developed for a tank with the experimental dimensions.

Table 4 shows different parameters used in the modeling of the tanks. m :total water mass, h_c :convective mass height, h_i : impulsive mass height, m_c : convective mass, m_i : impulsive mass, K_c : convective mass spring.

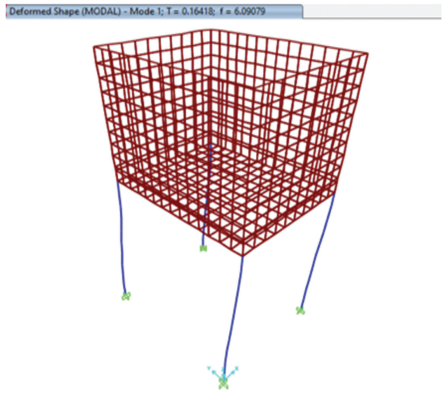

Fig.16 Frequency and period of the empty tank's first mode shape

Table 4 Convective and impulsive parameters used in modeling using the simplified method

Code	h_w (m)	m	h_c	h_i	m_c	m_i	K_c
Eurocode	0.014	0.65	0.7	0.56	0.53	0.12	24.3
	0.026	1.21	1.32	1.04	0.94	0.27	75.6
	0.038	1.77	1.97	1.52	1.28	0.49	139.2
	0.05	2.32	2.66	2	1.53	0.79	201.2
	0.061	2.83	3.33	2.44	1.71	1.13	249.5
	0.073	3.39	4.12	2.94	1.84	1.55	290.5
	0.086	4	5.02	3.53	1.94	2.05	322.3
	0.098	4.55	5.9	4.09	2	2.55	342.3
ECP	0.014	0.65	0.7	0.53	0.53	0.05	21.6
	0.026	1.21	1.3	0.99	0.95	0.19	62.7
	0.038	1.77	1.98	1.44	1.32	0.39	103.7
	0.05	2.32	2.6	1.9	1.62	0.65	166.4
	0.061	2.83	3.23	2.32	1.83	1.02	216.1
	0.073	3.39	4.02	2.77	2	1.44	259.3
	0.086	4	4.82	3.27	2.17	1.9	293.9
	0.098	4.55	5.88	3.72	2.27	2.48	322

Only the first two mode shapes have been taken into consideration as they had a cumulative mass participation factor of more than 99.999% as shown in Table 5.

Table 5 Mass participation of a tank partially filled with water (h=9.8 cm)

Steptype text	Stepmum unitless	Period sec	UX unitless	UY unitless	UZ unitless	SumUX unitless
Mode	1	0.506322	0.426225	0	0	0.426225
Mode	2	0.216678	0.573765	0	0	0.99999
Mode	3	0.163733	0	0.999987	0	0.99999
Mode	4	0.135182	0	0	0	0.99999
Mode	5	0.017159	0	0	0.000455	0.99999

In Table 6, a thorough comparison has been made between the sloshing frequencies calculated from the Eurocode-8 Part 4 equation, Egyptian Code of Practice (ECP), and the experimental frequencies measured via Digital Image Correlation (DIC) during the experiments in an elevated rectangular water tank at water heights ranging from 1.4 cm to 9.8 cm. The ranges of experimental sloshing frequencies ranged between 1.00 Hz and 1.84 Hz versus the Eurocode calculated frequencies of 1.07 Hz and 1.93 Hz, producing a percentage difference of 3.24% and 7.36%. As for ECP, the sloshing frequencies ranged between 1.01 Hz and 1.77 Hz, producing a percentage difference of 1.0%, and 9.21%. The errors in

Eurocode indicate the difficulty in using basic assumptions of circular tanks for rectangular geometries, since rectangular geometries have variations when it comes to boundary conditions and features of wave propagation. The maximum error of 7.36% at 5 cm was still under acceptable error according to the Eurocode. As discussed previously, potential nonlinear sloshing behavior, such as wave breaking or turbulent flow at higher water heights, is not computed in the simplified model.

Table 6 Eurocode results and comparison with lab results

Water height (cm)	Method	Impulsive frequency (Hz)	Difference (%)	Convective frequency (Hz)	Difference (%)
1.4	Experimental	5.84	--	1	--
	ANSYS	5.82	0.34	0.95	5
	Eurocode	5.8	0.68	1.07	7
	ECP	5.89	0.86	1.01	1
2.6	Experimental	5.67	--	1.32	--
	ANSYS	5.66	0.18	1.26	4.55
	Eurocode	5.69	0.35	1.41	6.82
	ECP	5.75	1.41	1.28	3.03
3.8	Experimental	5.29	--	1.52	--
	ANSYS	5.42	2.46	1.47	3.29
	Eurocode	5.47	3.4	1.62	6.58
	ECP	5.54	4.73	1.38	9.21
5.0	Experimental	5.11	--	1.63	--
	ANSYS	5.14	0.59	1.6	1.84
	Eurocode	5.23	2.35	1.75	7.36
	ECP	5.33	4.31	1.56	4.29
6.1	Experimental	4.94	--	1.76	--
	ANSYS	4.87	1.42	1.69	3.98
	Eurocode	4.99	1.01	1.83	3.98
	ECP	5.04	2.02	1.66	5.68
7.3	Experimental	4.45	--	1.82	--
	ANSYS	4.58	2.92	1.75	3.85
	Eurocode	4.73	6.29	1.88	3.3
	ECP	4.77	7.19	1.72	5.49
8.6	Experimental	4.3	--	1.85	--
	ANSYS	4.29	0.23	1.79	3.24
	Eurocode	4.46	3.72	1.91	3.24
	ECP	4.51	4.88	1.74	5.95
9.8	Experimental	4.01	--	1.84	--
	ANSYS	4.02	0.25	1.81	1.63
	Eurocode	4.24	5.74	1.93	4.89
	ECP	4.24	5.74	1.77	3.8

Table 6 highlights the simplified method's utility as a practical tool for preliminary design, offering reasonable estimates despite its simplifications, but also underscores its limitations compared to the higher accuracy of DIC (validated against ANSYS with errors up to 4.55% for convective frequencies). By measuring these differences, Table 6 supports the study's aim to evaluate simplified design codes against experimental and numerical procedures, offering important perspectives on the accuracy of the simplified method for rectangular tank design, and demonstrates that sophisticated techniques, for example DIC, are needed for accurate dynamic response analysis in seismic design.

Eq. (8) was used to create Table 7 which shows the difference between the equation of sloshing frequency of the rectangular tanks in the Euro-code and lab results. The maximum error of the sloshing frequency is 8%, which is considered reasonable.

Table 7 Comparison between lab results and the equation of the rectangle sloshing frequency in Eurocode

model	hw (cm)	Eurocode (exact rectangle equation) (Hz)	Error (Eurocode) (exact rectangle equation) (%)
1	1.4	0.92	8.00
2	2.6	1.23	6.82
3	3.8	1.44	5.26
4	5.0	1.60	1.84
5	6.1	1.70	3.41
6	7.3	1.79	1.65
7	8.6	1.85	0
8	9.8	1.89	2.72

3 Conclusions

This study experimentally and numerically investigated the natural frequencies of an elevated rectangular water tank that focusing on fluid-structure interaction. The methods enployed DIC, as an experimental measurement, ANSYS finite element analysis, and simplified models based on the Eurocode and Egyptian Code of Practice (ECP). The findings provide valuable information on the dynamic behavior of elevated tanks and validate the use of DIC as a non-contact measuring technique.

The experimental DIC data, recorded with a high-speed camera, were analyzed using CWT and FFT. The analysis showed that increasing the water height from 0 cm to 9.8 cm, decreased the impulsive frequency from 5.8724 Hz to 4.0085 Hz due to the added liquid mass, while the sloshing frequency increased from 1.00 Hz to 1.84 Hz, indicating greater wave motion. Observed results exhibited similar trends with the validation by ANSYS at each water height, producing a maximum error of 2.92% for impulsive frequencies and 5% for convective frequencies in comparison to the DIC results, indicating a high rate of numerical accuracy. The DIC results closely matched the ANSYS results to validate DIC as a useful method for measuring impulsive as well as convective modes of vibration, where minor errors in frequencies at 3.8 cm and 7.3 cm were attributed to camera frame rate capture limitations (240 Hz) or the level of resolution achieved from the speckle pattern.

The simplified models based on Eurocode and ECP provided practical alternatives for frequency estimation. The Eurocode sloshing model ultimately led to percentage errors of 6.29% and 7.36% for impulsive and convective frequencies, respectively, while ECP resulted in percentage errors of 7.19% and 9.21%, respectively. Both were less accurate than ANSYS. The sloshing frequency obtained using the Eurocode was developed from a model with assumptions based on circular tanks. The ECP model's larger errors were experienced especially at higher water levels and were ultimately due to the use of a simplified two-mass assumption in conjunction with graphical charts. Given that DIC and ANSYS have substantially higher accuracy than the simplified models discussed, these comparisons illuminate the difference between practical-useful results against the ill-posed limitations of simplifying assumptions. Advanced methods are needed in such a critical application.

The practical implications of this study are significant for structural engineering. The validated DIC method offers a cost-effective, non-contact approach to measure dynamic responses, enabling engineers to assess tank behavior under seismic loads with high accuracy. This is crucial for designing and monitoring elevated rectangular tanks in earthquake-prone regions, where resonance avoidance is paramount. The Eurocode's reasonable accuracy supports its use in preliminary design phases, while ANSYS's reliability is ideal for detailed analyses requiring precise frequency predictions. However, the study's limitations must be considered. The small-scale tank model may not fully replicate the behavior of full-scale structures, where additional factors like soil-structure interaction or larger wall dimensions could influence dynamics. The DIC setup's reliance on a 240 Hz camera may have missed transient high-frequency phenomena, and the speckle pattern's resolution could introduce minor errors in displacement tracking, particularly at higher water levels where turbulent flow complicates measurements. Additionally, the simplified models' assumptions, especially for rectangular geometries, limit their accuracy in capturing complex fluid-structure interactions.

Future research should address these limitations by applying DIC to full-scale tanks under real seismic excitations to evaluate its scalability. Incorporating higher-frame-rate cameras or advanced image processing could enhance DIC's ability to capture high-frequency modes. Exploring soil-structure interaction effects, as suggested by Visuvasam et al.[7], could provide a more

comprehensive understanding of tank dynamics in diverse geotechnical conditions. Further refinements to simplified models, such as tailored equations for rectangular tanks or integration of nonlinear sloshing effects, could improve their reliability. Additionally, investigating the impact of internal baffles, as studied by Kangda et al.[9], on rectangular tank frequencies could inform design strategies to mitigate sloshing amplitudes. These advancements would build on this study's foundation, enhancing the safety and efficiency of elevated tank designs in seismic zones.

References

[1] Sahu D K, Gupta H, Dev N, et al. A comparative analytical and experimental analysis of sloshing waves in a rectangular tank under seismic conditions. International Journal of Research in Engineering and Technology, 2016, 5(6): 319-324. DOI:10.15623/IJRET.2016.0506058.

[2] Rayleigh L. The Theory of Sound. Cambridge: Cambridge University Press. 1945.

[3] Timoshenko S P, Gere J M, Young D H. Theory of Elastic Stability. New York: McGraw-Hill Education. 2012.

[4] Clough R W, Penzien J. Dynamics of Structures. New York: McGraw-Hill Education. 2003.

[5] Pal P, Bhattacharyya S. Sloshing in partially filled liquid containers— Numerical and experimental study for 2-D problems. Journal of Sound and Vibration, 2010, 329(21): 4466-4485. DOI: 10.1016/j.jsv.2010.05.006.

[6] Ninan S, Hameed A. Seismic analysis of rectangular and circular RC elevated water tank. International Journal of Engineering Research & Technology, 2018, 6(6): 1-4.

[7] Visuvasam J, Simon J, Packiaraj J, et al. Seismic response of elevated rectangular water tanks considering soilstructure interaction. IOP Conference Series: Materials Science and Engineering, 2017, 263(3): 032036. DOI: 10.1088/1757-899X/263/3/032036.

[8] Vimal P, Regin J, Jinu G, et al. Experimental investigation on elevated water tanks with base isolation—response spectrum approach. Journal of Theoretical and Applied Mechanics, 2020, 58(4): 885-899. DOI: 10.15632/jtam-pl/125617.

[9] Kangda M Z, Raikar R G, Wadki V. Sloshing phenomena in square water tanks with internal obstructions using fluid dynamics. Structural Engineering Convention. Berlin: Springer, 2023, 1-9. DOI:10.1007/978-981-97-9885-8_1.

[10] Fang X, Bao X, Yue F, et al. A dynamic analysis method of liquid-filled containers considering the fluid-structure interaction effect. Applied Sciences, 2024, 14(7): 2688. DOI:10.3390/app14072688.

[11] Sun Y, Meng X, Zhang Z, et al. Liquid sloshing in soil-supported multiple cylindrical tanks equipped with baffle under horizontal excitation. Buildings, 2024, 14(4): 1029. DOI:10.3390/buildings14041029.

[12] Meng W, Bachilo S M, Weisman R B, et al. A review: Non-contact and full-field strain mapping methods for experimental mechanics and structural health monitoring. Sensors, 2024, 24(20): 6573. DOI:10.3390/s24206573.

[13] Montiel F, Bonnefoy F, Ferrant P, et al. Hydroelastic response of floating elastic discs to regular waves. Part 1. Wave basin experiments. Journal of Fluid Mechanics, 2013, 723: 604-628. DOI:10.1017/jfm.2013.123.

[14] Kumar D, Chiang C H, Lin Y C. Experimental vibration analysis of large structures using 3D DIC technique with a novel calibration method. Journal of Civil Structural Health Monitoring, 2022, 12: 391-409. DOI: 10.1007/s13349-022-00549-5.

[15] Zhang M, Schreier S, Hopman H. Digital image correlation application to a modular flexible floating structure. Proceedings of the International Ocean and Polar Engineering Conference. Cupertino: International Society of Offshore and Polar Engineers, 2020, 1039-1046.

[16] Zhang P, Carretto A, Porfiri M. Simultaneous digital image correlation/particle image velocimetry to unfold fluid-structure interaction during air-backed impact. Journal of Fluids and Structures, 2020, 95: 102980. DOI: 10.1016/j.jfluidstructs.2020.102980.

[17] Luo X, Zhang S, Li A, et al. Steel rebar effect on tensile and cracking behavior of UHPFRC based on direct tensile tests and digital image correlation. Cement and Concrete Composites, 2023, 137: 104940. DOI: 10.1016/j.cemconcomp, 2023.104940.

[18] Aryanto A, Revolis M, Oribe Y, et al. Application of digital image correlation method in RC and FRC beams under bending test. International Journal of GEOMATE, 2023, 24(101): 118-125. DOI: 10.21660/2023.101.g12275.

[19] Anagha B V, Nimisha P, Jayalekshmi B R. A study on effect of fluid on the modal characteristics of ground-supported water tanks. International Conference on Materials, Mechanics and Structures. Bristol: IOP Publishing, 2020, 936(1): 012027. DOI:10.1088/1757-899X/936/1/012027.

[20] European Commission. Eurocode 8: Design of structures for earthquake resistance-Part 4: Silos, tanks and pipelines. EN 1998-4: 2006. https://eurocodes.jrc.ec.europa.eu/EN-Eurocodes/eurocode-8-design-structures-earthquake-resistance.

[21] Egyptian Code Committee. Egyptian code for estimating loads and forces in structural and construction works (Code 201). 2012.

[22] Rashed A A, Mahmoud G H, Nasr N E, et al. 3D analysis for conical tanks under seismic loads. Journal of Mechanical and Civil Engineering, 2019, 16(1): 29-44. DOI: 10.9790/1684-1601012944.